Investigation of Heaterless Hollow Cathode Breakdown

IEPC-2015-193

Presented at Joint Conference of 30th International Symposium on Space Technology and Science
34th International Electric Propulsion Conference and 6th Nano-satellite Symposium,
Hyogo-Kobe, Japan
July 4 – 10, 2015

Alexander Daykin-Iliopoulos [1], Steve Gabriel[2] and Igor Golosnoy[3]
University of Southampton, SO17 1BJ, United Kingdom

Kenichi Kubota[4]
Japan Aerospace Exploration Agency, Chofu, Tokyo, 182-8522, Japan

Ikkoh Funaki[5]
Japan Aerospace Exploration Agency, Sagamihara, Kanagawa, 252-5210, Japan

Abstract: The development of long life high powered (>50A) hollow cathodes is of importance to meet the demand of increasingly powerful Gridded Ion engines and Hall Effect thrusters. High power cathodes typically operate at greater temperature ranges, which poses a significant challenge to maintain heater reliability. The heater component commonly used to raise the insert to emissive temperatures, has inherent reliability issues from thermal fatigue caused by thermal cycling with large temperature variations. A self-heating hollow cathode allows for potentially higher reliability through design simplicity of removing the heater component, and in addition there can be savings in mass, volume, ignition time and power. This study characterizes the initiation of the start-up process for a heaterless hollow cathode. As such the study analyses conditions of the initiation as a function of detailed geometrical and physical parameters. The Paschen curve can be seen to give a qualitative explanation for the breakdown voltage variance. The quantitative variations between the empirical results and Paschen curve are discussed in relation to non-uniform pressure simulations.

Nomenclature

HHC	=	heaterless hollow cathode
sccm	=	standard cubic centimeter
M_a	=	atomic mass
mg/s	=	milligrams per second
LaB_6	=	lanthanum hexaboride

I. Introduction

The steady operation of thermionic hollow cathodes (HCs) depends on thermionic current which in turn requires high temperatures of the HC's insert, above 1500 K. For the hollow cathode ignition a common solution is to use a heater to raise the insert temperature up to these emissive temperatures, however this has drawbacks: 1) additional mass and volume due to the heater, 2) reliability issues, and 3) delayed ignition (large response times). Hence it would

[1] PhD Student, Tony Davies High Voltage Laboratory, Alexander.Daykin-Iliopoulos@soton.ac.uk.
[2] Professor, Tony Davies High Voltage Laboratory, sbg2@soton.ac.uk.
[3] Associate Professor, Tony Davies High Voltage Laboratory, ig@ecs.soton.ac.uk.
[4] Researcher, Institute of Aeronautical Technology, kubota.kenichi@jaxa.jp
[5] Associate Professor, Institute of Space and Astronautical Science, funaki@isas.jaxa.jp

be beneficial to remove the heater and to replace it with a simpler and potentially faster ignition system. It is known that standard hollow cathodes can be started from cold by passing very high flow rates and applying high voltages to the keeper but such an approach can lead to unacceptable losses of propellant and strong erosion[1].

We are developing a prototype hollow cathode which eliminates the need for a heater. In our proposed system, the ignition (and consequent heating of the HC's insert) is driven by a discharge between the keeper and the cathode. Such that the insert is raised to the equilibrium thermionic temperatures by the discharge itself rather than requiring an additional heater component. The heaterless hollow cathode (HHC) ignition undergoes three main stages, to transition from dormant to nominal operation: breakdown, heating, and keeping[2,3]. Initiation of one stage does not guarantee progression to the next stage(s)[1,4], such that breakdown or heating alone is not full ignition. Low power heaterless ignition of relatively low work function inserts such as lanthanum hexaboride is possible[5] as well as impregnated tungsten sponge with barium scandate[6]. Additionally there is indication that the erosion rate of heaterless ignition is comparable to heated ignition[7]. The ignition voltage depends on the shape of the system components as well as the gas pressure field, experiments have shown the effects of geometric variations for heated ignition[8]. The overall gas and geometric influence can be modelled by the Paschen law, meaning the keeper-cathode orifice distance and gas pressure has an optimum product at which the breakdown voltage is minimum. This is essentially a good zeroth order model, however due to neither conditions of the standard Paschen law[9] being satisfied (static pressure and parallel plate geometry), it may not be adequate for the design of a reliable ignition. So for reliable and repeatable heaterless ignition, an investigation of the detailed geometric features, which in turn determine the electric field and pressure distribution which influence the ignition is required. As such this study analyses conditions of the ignition as a function of detailed geometrical and operational parameters such as keeper voltage and mass flow rate.

The experimental apparatus including the electrical and flow management set-up is described in section two of this paper. Section three depicts the design of our heaterless hollow cathode, including outlining the main differences in comparison to conventional hollow cathodes. Then the results and discussions are presented in section four, this section is discretized into the sub-categories of our investigation of the heaterless hollow cathodes breakdown including: influence of cathode keeper distance, influence of detailed geometry changes, experimental repeatability, flow simulations and preliminary Paschen curves. Finally the conclusions are summarized in section five.

II. Experimental Apparatus

The experiments in this study where conducted in a 0.4 m^3 stainless steel vacuum chamber. An Edwards E2M80FX two stage vacuum pump was used to reduce base pressure to ~ 3×10^{-3} mbar at which point a Pfeiffer Balzers TPH 450H turbo pump lowered and maintained a base pressure of ~ 2×10^{-5} mbar. Throughout experimental operation a back pressure below ~ 5×10^{-3} mbar was maintained. The chamber pressure was measured by a Pfeiffer Balzers IKR-020 Penning gauge and a TPR 010 Pirani gauge, displayed on a TPG-300 vacuum gauge controller. An Edwards AIM-S-NW25 Active Inverted Magnetron Gauge was used with an Active gauge controller as an additional reference.

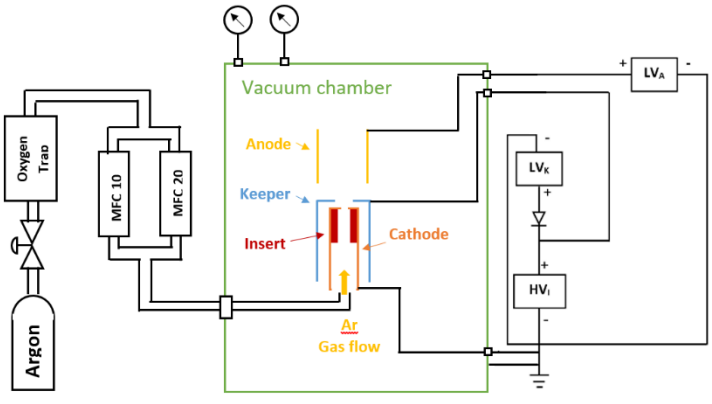

Figure 2: Schematic of the electrical and propellant setup

Figure 1: Photograph of experimental setup

Typically lower than 10% difference between gauge readings was seen. The overall equipment arrangement and chamber can be seen in Figure 1.

Argon was used for the duration of this study, the argon supply was controlled by two Bronkhurst EL-FLOW mass flow controllers with 0-10 sccm and 0-20 sccm flow rate ranges. They were connected though an oxygen trap to purify the supply. The combined flow rate controllers gave a maximum flow rate of 30 sccm to the HHC. The mass flow rate controllers where connected to a PC to which they were controlled by LABView software. A Tektronix DPO3034 Digital Oscilloscope, 300MHz, 2.5 Gsps, was used to measure the current and voltage from the power supply. A Glassman series FC high voltage power supply was equipped that could produce up to 1.5kV, 80mA, to the keeper. A schematic of the propellant and electrical arrangement can be seen in Figure 2, for this study the Anode was not used as the breakdown investigated was between the cathode-keeper electrodes.

III. Heaterless Hollow Cathode Design

We have designed and built a 20A heaterless hollow cathode as an evolving step towards the design and operation of high-powered (>50A) HHC's. As such this prototype cathode allows for quick modification of key geometric parameters including the cathode-keeper distance, keeper orifice, and cathode orifice. The schematic overview of the LaB6 heaterless hollow cathode can be seen in Figure 3, and the dissembled parts are shown in Figure 4.

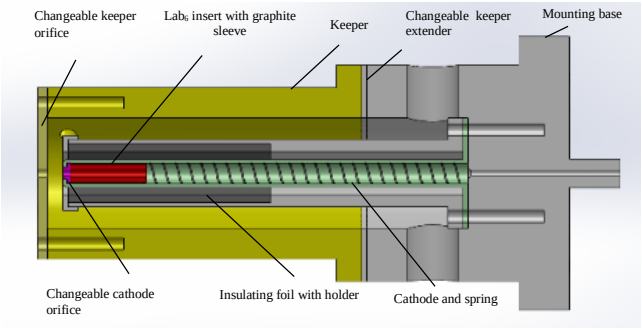

Figure 3: Schematic of the LaB_6 heaterless Hollow cathode

It can be seen that the overall components within our heaterless hollow cathode are in common with conventional heated hollow cathodes, including: cathode, keeper, multilayered insulation and low work insert. The main difference being the removal of the heater component and detailed geometry changes to the keeper and cathode orifices which will be discussed in Section IV.

Figure 4: Heaterless hollow cathode disassembled

The heaterless hollow cathode consists of a 30 mm thick macor base which electrically and thermal insolates the HHC. A molybdenum tube 80 mm in length with a 4.9 mm inner diameter is secured to the base. A 0.75 mm long graphite cathode orifice is inserted into the tube. Separating the orifice from the cathode tube allows for quick modifications to the cathode orifice. The orifice is followed by the lanthanum hexaboride (Lab_6) insert with an inner diameter of 2 mm with an outer diameter of 4.5 mm, and a length of 15 mm, which has been provided by Lanzhou Institute of Physics. The insert is covered in a 0.2 mm graphfoil sleeve, to electrically connect yet mechanically separate the Lab_6 insert from the refectory tube, due to the known issues of boron diffusion[9]. The flexible graphfoil allows for a close fit with the Lab6 insert when inserted into the molybdenum tube, and its compressible properties delivers good contact while undergoing thermal expansion, such that mechanical stresses on the insert are minimized. The insert was held in place with a tungsten spring. A stainless steel casing will be used to support the multilayered tantalum thermal shielding that will aid in raising the HHC to operational steady-state temperatures.

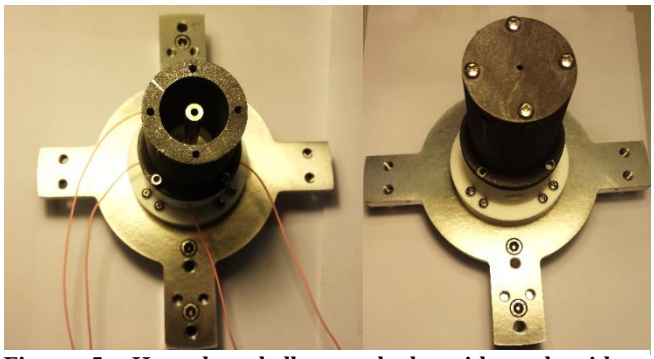

Figure 5: Heaterless hollow cathode with and without changeable keeper orifice

The enclosed graphite keeper is secured to the macor base with a graphite keeper extender in-between, used to vary keeper cathode distance. The keeper orifice is secured to the keeper end of the keeper (see Figure 5), once again this is to allow quick alteration to this keeper orifice. The propellant tube line was attached to the rear macor base using an Ultra-Torr Swagelok fitting to provide a leak free seal to the ceramic.

IV. Results and discussions

A. Influence of the keeper cathode separation

The breakdown voltage of the hollow cathode was determined by steadily increasing the ignition voltage until a discharge was observed by a rapid voltage drop and rise in current seen on the oscilloscope. Simultaneously the discharge was visibly seen originating from the keeper orifice through the chamber window. At each breakdown the data was logged and the voltage re-set to a low value before again steadily increasing to the breakdown voltage. This was repeated 10 times at 7 different flow rates from 1 to 30 sccm. This was conducted for three different keeper-cathode separations. As previously mentioned the separation was increased through a series of graphite keeper extenders to increase the enclosed keeper's length. The results can be seen in Figure 6, note for most data points the standard deviation is smaller than the marker size. Breakdown was not achieved for the 1mm separation below 5 sccm, and also for the 11mm separation below 2 sccm, such that the breakdown voltage at those conditions must have been higher than the available maximum output of the 1.5kv power supply.

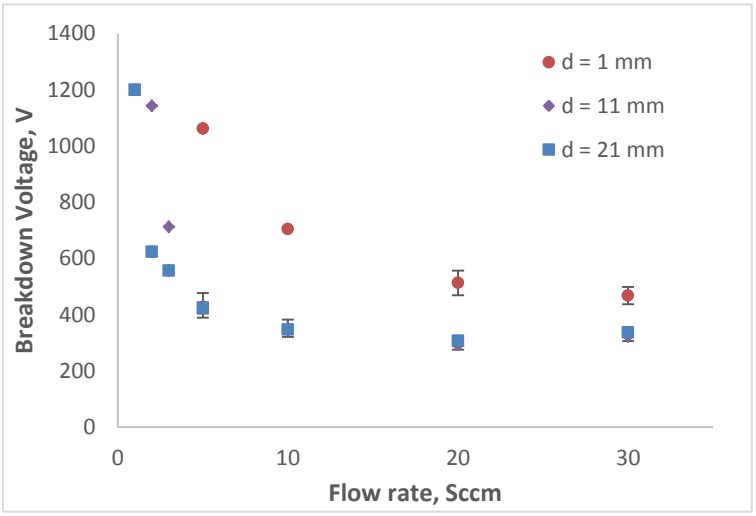

Figure 6: Varying cathode-keeper gap, 2 mm keeper orifice and 1.2 mm cathode orifice data labels showing the simulated pressure.

As the flow rate is increased the breakdown voltage drops, this is more significant in the low flow rate range - as would be expected from the Paschen curve. Additionally this has been observed by researchers[3] although for a different set-up (using xenon and with an isolated insert). Increasing the keeper-cathode separation resulted in reduced breakdown voltage at a given flow rate and reduces the flow rate at which the minimum breakdown voltage occurs. The breakdown voltage can be seen to be heavily impacted by the flow rate which provides a given pressure in the cathode-keeper gap region, from 1200 V at 1 sccm to 300 V at 20 sccm for the 21 mm gap (see Figure 6).

B. Keeper geometry modifications

Keeper orifices with detailed geometry modifications have been tested to examine their influence on the breakdown voltage of the heaterless hollow cathode. The modification decreases the radius of curvature on the keeper orifice with the intention of increasing the electric field strength, this is referred to as the sharp keeper orifice, see Figure 7. The sharp keeper was initially tested with the sharp edge towered the cathode, and then tested with it reversed so that the sharp edge is directed away from the cathode.

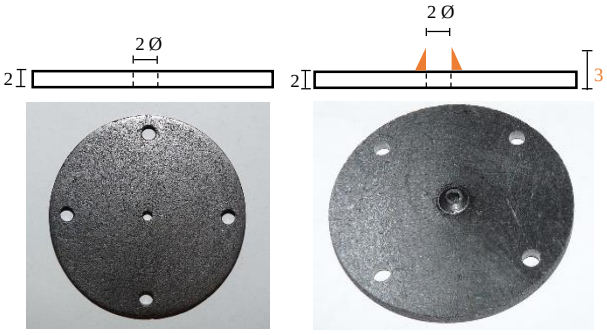

Figure 7: original 2 mm keeper (left), sharp keeper orifice with side view schematic above, dimensions in mm

The results of the different geometry orifices are shown in Figure 8. The breakdown voltage was determined in the same way as section IV A, with 10

breakdowns at each flow rate. It can be seen that the detailed geometry modifications have more influence on the breakdown voltage at lower flow rates. The sharp keeper orifice had a reduction in the mean breakdown voltage of 20 percent for 2 sccm in comparison to the original keeper orifice, the direction of the sharp keeper orifice did not appear to alter the breakdown voltage significantly.

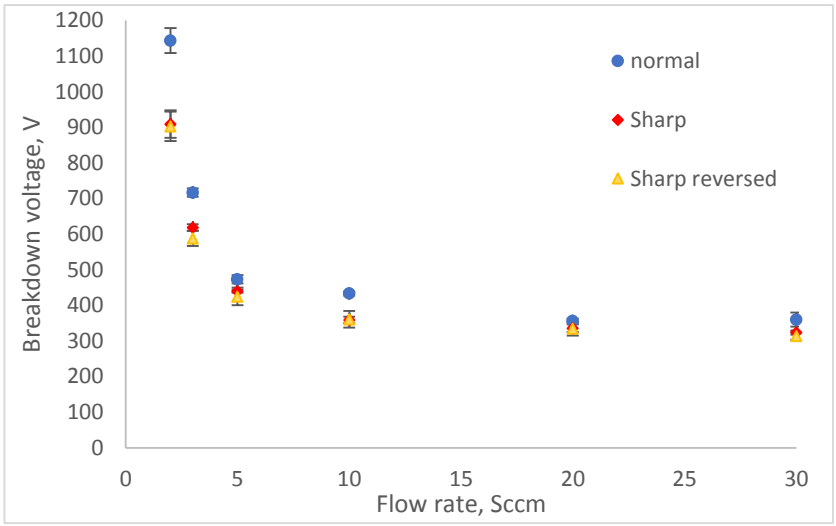

Figure 8: Breakdown voltage variation with keeper orifice modifications, cathode orifice diameter 1.5 mm, keeper orifice diameter 2 mm, 11 mm gap

C. Cathode geometry modifications

Three separate cathode orifices where designed and manufactured, the first a 1.5 mm inner diameter orifice. The second the same detailed geometry although with an increased inner diameter of 2 mm. The third was also 2 mm inner diameter although extruded (towered the keeper) by approximately 0.3 mm to a relatively small radius of curvature, referred to as the 2 mm sharp cathode orifice. All three orifices can be seen in Figure 9, with the breakdown results plotted in Figure 10. The 1.5 mm cathode orifice yields the lowest breakdown voltage at each flow rate. Comparing the 2 mm and 2 mm sharp cathode orifices it can be seen that the breakdown voltage of the sharp geometry is between 20-30 V lower for flow rates higher than 3 sccm. As the 2 mm sharp out-performed the standard 2 mm but the 1.5 mm demonstrated the lowest breakdown voltage, this indicates that a desirable geometry would be a 1.5 mm sharp, or of even smaller inner diameter with a sharp geometry.

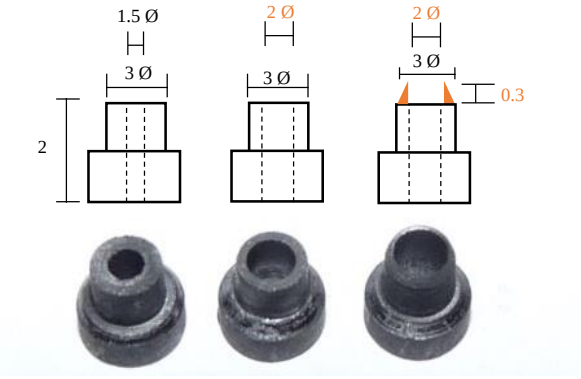

Figure 9: 1.5 mm cathode orifice (left), 2 mm cathode orifice (middle), and 2mm sharp cathode orifice (right), with side view schematic above, dimensions in mm

When comparing the results of the keeper orifice geometry modifications with that of the cathodes orifices there is an indication that the detailed keeper geometry and corresponding electrostatic properties have more influence on the breakdown voltage, due to the much higher reductions in breakdown voltage. The breakdown is initiated through a cascading avalanche of ionization that would be expected to initiate from the cathode, due to the positive polarity applied to the keeper. Such that an increase to the cathodes electric flied strength would decrease the voltage required to meet the conditions necessary to initiate the propagating ionization avalanche, hence the results that the keepers electric flied has higher influence are opposing to the understood mechanism of this breakdown. Hence perhaps the differences in the nominal length due to the extrusion

length for both the sharp keeper and cathode geometries (with the keeper geometry extruded by 1 mm, 0.7 mm more than the cathode by 0.3 mm) can explain some of the differences seen in the influence of the respective electrostatics. That said the separation for these tests is 11 mm, such that there is relatively small differences in the distance. Additionally it must be noted that the extrusions for sharp geometries effectively changes the aspect ratio of the orifice (length to radius ratio), and hence the corresponding flow profile will be changed, which can influence the breakdown voltage by the pressure differences caused.

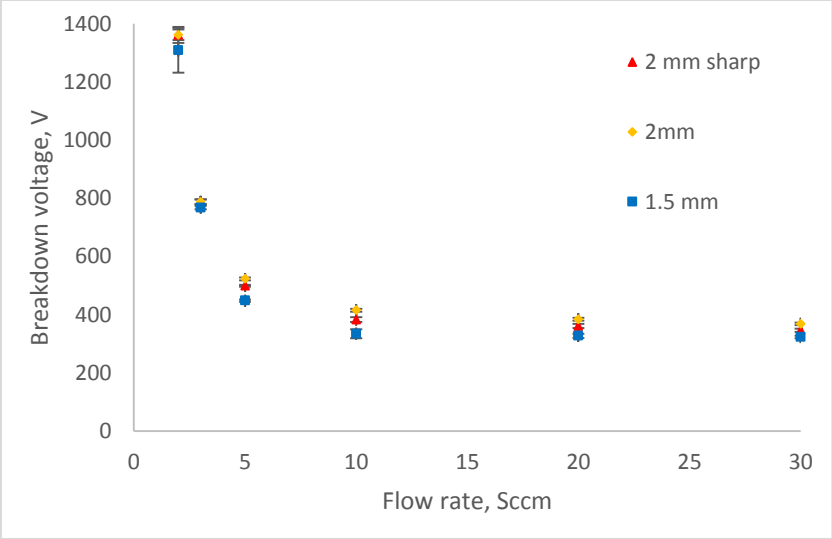

Figure 10: breakdown voltage variation with cathode orifice, keeper orifice diameter 2 mm, cathode keeper gap size of 11 mm

D. Repeatability

The repeatability of the breakdown voltage was examined by re-testing at each gap size for 3 separate rounds. The first round was repeated 10 times at each flow rate, with the flow rates in a random order. The second round was from lowest to highest flow rate, and the third was in reverse order. The second and third round where repeated 3 times at each flow rate. The results are plotted in Figure 11. It can be seen that the results overall have a small deviation in respect to the ordering of the runs.

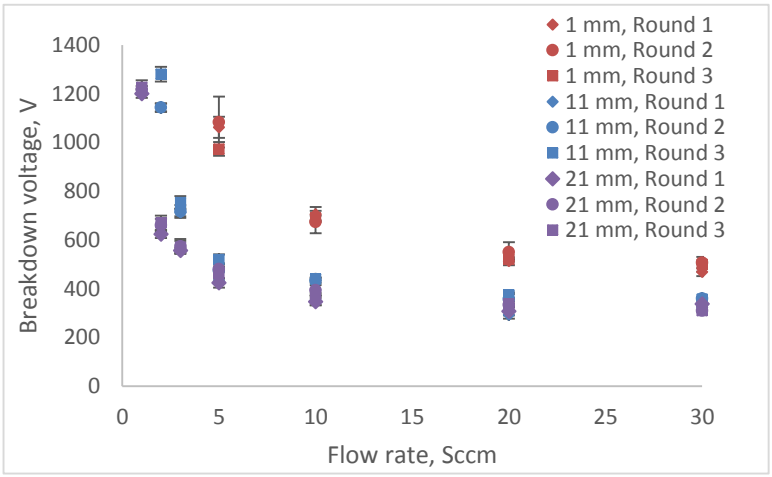

Figure 11: Repeatability tests, cathode orifice diameter 1.5 mm, keeper orifice diameter 2 mm

The standard deviation of the breakdown voltage for the combined runs is greater at lower mass flow rates, for example, 65 for 5 sccm compared with 25 for 20 sccm at the 1 mm gap. This is due to high gradient in the rejoin of the curve, such that a small deviation in pressure induces larger differences in the breakdown voltage. The standard deviation is smaller for larger separations, such that for 21 mm gap at 5 sccm the standard deviation is 30 and 20 at 20 sccm. Such that when comparing the 1 mm and 21 mm gap standard deviations stated above, there is an indication that greater flow stability is achieved with greater separation between the electrode orifices.

E. Flow simulations

To better understand the influence of pressure and the corresponding mass flow rates on the breakdown voltage, neutral flow simulations has been conducted to see the effect of varying geometrical parameters and mass flow rates on the neutral pressure field. The neutral flow analysis was carried out using a Direct Simulation Monte Carlo (DSMC) code[11]. The numerical campaign consisted of varying key geometric parameters to induce variations in the pressure profile. Though the pressure of the neutral flow is not uniform throughout the internal hollow cathode rejoins as can be seen in Figure 13. Hence the average pressure between the cathode-keeper orifice edges is calculated to compare against varying geometric parameters.

To acquire a first order analytical approximation the 20 sccm argon volumetric flow rate is converted to mass flow rate. From Goebel[12] it is shown that $1\ sccm\ =\ 7.43583 \times 10^{-4}\ m_a\ [\frac{mg}{s}]$, therefore 20 sccm argon with an atomic mass of 39.95, is equivalent to 0.594 mg/s (corrections for argon compressibility stands negligible for this calculation). As mass is conserved at steady state operation, 0.59 mg/s is the flowrate through the keeper orifice. Given the

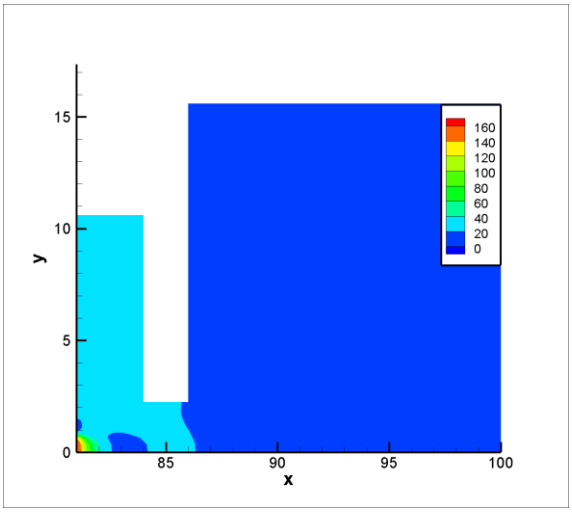

Figure 13: DSMC simulation of heaterless hollow cathode, 20 sccm, 4.5 mm keeper orifice, 1.5 mm cathode orifice, 3 mm gap

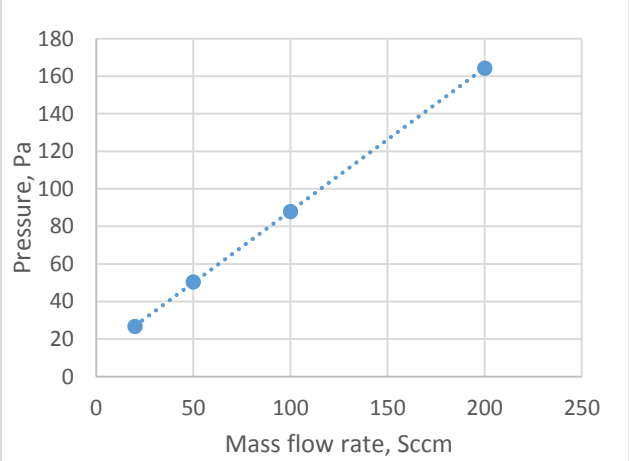

Figure 12: Pressure variation with flow rates, 3 mm gap, 1.5 mm cathode orifice and 4.5 mm keeper orifice.

following known information: mass flowrate passing though the keeper orifice of 0.59 mg/s, the keeper orifice radius of 2.25 mm, and the back pressure of ~ 0 pa. Then assuming a gas temperature in the order of 300 K and approximating the keeper orifice length to radius ratio to 1, using[13,14] gives the pressure within the cathode keeper gap to be ~ 24 pa. Although this simplistic analytical approach does not take into account the complex flow regimes of the two orifice system it has give an approximation within 10 % of the simulated average pressure between the two orifices, which was 26.6 pa, seen in Figure 12.

Figure 12 quantifiably shows the average pressure between the electrode edges is directly proportional to the flow rate as would be expected due to the conservation of mass through the system. Simulations have also determined the influence on mean pressure in the cathode keeper cavity with varying the cathode-keeper gap Figure 14 and varying the keeper size Figure 15. It can be seen that both variations do not have a linear relationships to the average pressure. Thus when maximizing pressure to lower breakdown voltage for a given flow rate, the pressure trends indicate maximizing the gap distance and reducing the keeper orifice size, though combined changes to gap and keeper orifice will have a combining geometric effect to the flow profile that is not easily extrapolated from the individual trends shown. Additionally it is prudent to acknowledge that such design changes can limit performance of the hollow cathode when fully running, hence would require a trade-off with the breakdown voltages.

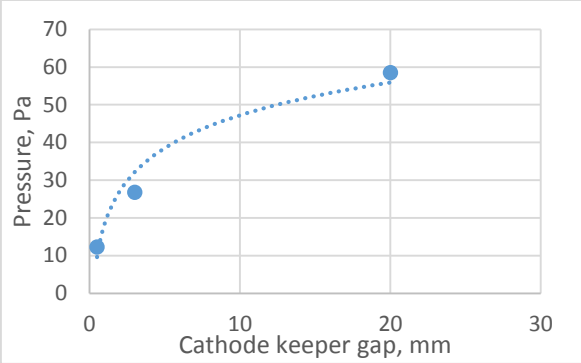

Figure 14: Pressure variation with cathode-keeper gap, 20 sccm flow rate, 1.5 mm cathode orifice and 4.5 mm keeper orifice.

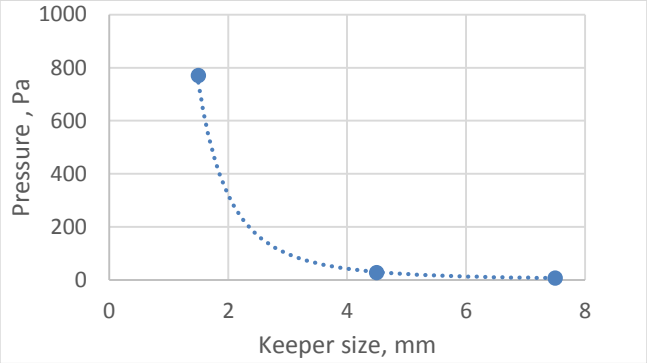

Figure 15: Pressure variation with keeper orifice size, 20 sccm flow rate, 3 mm gap, 1.5 mm cathode orifice

F. Preliminary Paschen curves

The Paschen curve has been used as a zeroth order model, however as previously mentioned due to neither the static pressure nor parallel plate geometry conditions of the standard Paschen law being satisfied it cannot be assumed to fully represent this system. Hence using the pressure simulations conducted and extrapolating for the varying flow rates, the average pressure from cathode-keeper edges has been estimated for the of the empirical results shown in Figure 6, these pressures are multiplied by the respective gap distances and plotted in Figure 16. Note as the simulations have a high computational cost, the 21 mm gap simulation was uncompleted at the time of writing this paper hence it is not shown in Figure 16. This Figure also plots the theoretical[9] and experimentally found Paschen curves by other researchers[15] for argon.

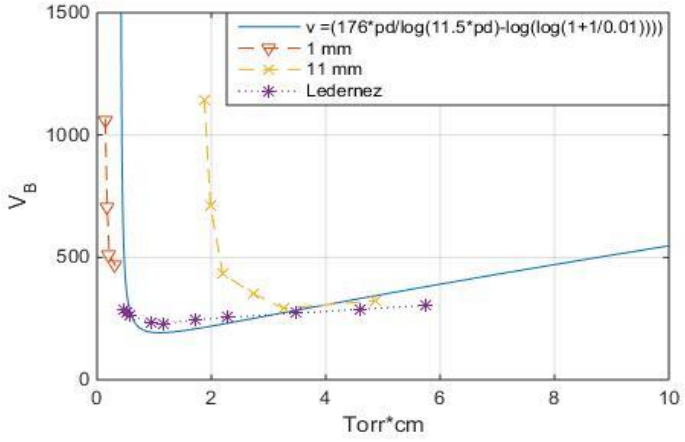

Figure 16: Paschen curves for 1 mm & 11 mm gaps, with additional theoretical[9] and experimental[15] curves plotted for reference

The Paschen shape is clearly depicted with the 1 mm and 11 mm, although a transition to the right is apparent. This transition is likely due to neither the static pressure nor parallel plate geometry conditions of Paschen breakdown being met in our system. Additionally as shown in Figure 14, the separation influences pressure such that pressure and distance are not independent variables within our system. The distance used in the calculations is the nominal distance between electrodes. The electric flied strength is strongest at the cathode and keeper orifices the discharge would be expected to follow such an equipotential path, though the discharge may not take this path in practice.

V. Conclusion

It has been shown quantifiably that the cathode to keeper orifice distance and argon flow rates with the corresponding cathode keeper cavity pressures are key parameters in the breakdown voltage,. The breakdown voltage variation with these parameters has been characterized. Additionally it was found that changes to the detailed geometry of the keeper orifice can influence the breakdown voltage, namely the alterations to the radius of curvature can lower the breakdown voltage by up to 20%. The effect of the cathode orifice geometry was far less significant than that of

the keeper geometry. Repeatability experiments have demonstrated, that although breakdown is stochastic in nature as expected, there are small variations in the breakdown voltage for given parameters in regards to prior tests. There is a preliminary Paschen curves plotted from the experimental and simulated results and compared with the theoretical and experimentally found Paschen curves for argon, which shows pd transitions in relation to the cathode keeper separations.

Investigation of the parameters influencing the next phases in the hollow cathode ignition, namely the heating to thermionic temperatures and then the final stable discharge, will allow for the effective design of high powered heaterless hollow cathodes. As well as SEM, and experimental pressure measurements to verify the gap change influence on the Paschen curve. Additionally spectrographic data will be collected and analyzed to aid in determining erosion parameters.

Acknowledgments

The authors would like to express their gratitude to the Tony Davis High voltage laboratory for their assistance in the fabrication of this heaterless hollow cathode, facility set-up and consistent lab support. In addition the authors would thank Juan Li and Yanhui Jia for providing valuable experimental assistance, as well as guidance from there past electric propulsion experiences. Finally the authors would like to thank the Lanzhou Institute of Physics, for providing the lanthanum hexaboride insert for our heaterless hollow cathode.

References

[1] Aston, G., "Ferm cathode operation in the test bed Ion Engine", 17th International Electric Propulsion Conference, Tokyo, Japan, May 28-31, 1984.
[2] Vekselman V., et al., "Characterization of a Heaterless Hollow Cathode", Journal of Propulsion and Power, Vol. 29, No. 2, pp. 475-486, March–April, 2013.
[3] Schatz M. "Heaterless ignition of inert gas ion thruster hollow cathodes", 18th International Electric Propulsion Conference, Alexandria, VA., USA, September 30-October 2, 1985.
[4] Vekselman V., et al., "A comparative study of heaterless hollow cathode: 2D PIC modeling vs. experiment", 33rd International Electric Propulsion Conference, Washington, D.C., USA, October 6-10, 2013.
[5] Albertoni R., et al., "Preliminary Characterization of a LaB6 Hollow Cathode for Low-Power Hall Effect Thrusters", 33rd International Electric Propulsion Conference, Washington, D.C., USA, October 6-10, 2013.
[6] Koshelev N., et al., "Investigation of hollow cathode for low power hall effect thruster", 30th International Electric Propulsion Conference, Florence, Italy, September 17-20, 2007.
[7] Arkhipov B., "Development and Research of Heaterless Cathode-Neutralizer for Linear Hall Thrusters (LHD) and Plasma Ion Thrusters (PIT)" 25th International Electric Propulsion Conference, Oct, Cleveland, Ohio, 1997.
[8] Fearn, D. and Patterson, S., "The Hollow Cathode - A Versatile Component of Electric Thrusters" Spacecraft Propulsion, Third International Conference, Cannes, France, 10-13 October, 2000.
[9] Lieberman A., Lichtenberg A., "Principles of plasma discharges and materials processing", Wiley, 2nd edition, 2005.
[10] Goebel D., Chu E., "High-Current Lanthanum Hexaboride Hollow Cathode for High-Power Hall Thrusters", Journal of Propulsion and Power, Vol. 30, No. 1, pp. 35-40, 2014.
[11] Kubota1 K., et al., "Hybrid-PIC Simulation on Plasma Flow of Hollow Cathode", 34th International Electric Propulsion Conference, Kobe, Japan, July 4-10, 2015.
[12] Goebel, D., and Katz, I., "Fundamentals of Electric Propulsion: Ion and Hall Thrusters", Willy, Hoboken, NJ, pp. 243-315, 2008.
[13] Sharipov F., "Numerical simulation of rarefied gas flow through a thin orifice", Journal of Fluid Mechanics, 518, pp 35-60., 2004.
[14] Varoutis, S. and Valougeorgis, D. and Sharipov, F., "Simulation of gas flow through tubes of finite length over the whole range of rarefaction for various pressure drop ratios", Journal of Vacuum Science & Technology A, 27, pp 1377-1391, 2009.
[15] Ledernez L., Olcaytug F., Urban G., Inter-Electrode Distance and Breakdown Voltage in Low Pressure Argon Discharges", Contributions to Plasma Physics, Vol. 52, Issue 4, pp 276–282, May 2012.